Practical Self-Testing

The application of self-testing techniques to experimental data

Lee Zhi Xian

Supervisor: Prof. Valerio Scarani

A thesis presented in partial fulfillment of the requirements of the degree of Bachelor of Science with Honours

Department of Physics
National University of Singapore

9 April 2018

Acknowledgements

The completion of this project would not have been possible without the guidance of Professor Valerio Scarani and his PhD student Goh Koon Tong. They have taught and clarified many important concepts during the numerous consultation sessions I have had with them, and have consistently monitored my progress over the duration of the project. I would hence like to express my gratitude for the time and support generously given to me throughout the course of this project. Also, I would like to thank Cai Yu for his help with Matlab issues.

Contents

1 Introduction

The main focus of this project revolves around the idea of Self-Testing, which is in essence the fact that the observation of *some* correlations, one can identify a quantum state and measurements on that state (up to local unitaries and addition of irrelevent degrees of freedom) which would give those correlations. An example would be that the observation of $CHSH = 2\sqrt{2}$ (the maximal violation possible of the CHSH inequality[3, 11] assuming quantum theory) self-tests[1] the singlet state, with the measurements being the corresponding sigma matrices.

The nature of Self-testing is such that it only works in the ideal or perfect scenario, when one observes the perfect correlations (for example $CHSH = 2\sqrt{2}$). To make it applicable to real data, one needs to allow for some deviation from the perfect case ($CHSH = 2\sqrt{2}-\epsilon$). In such situations, the lower bound of the fidelity with the ideal state is determined using what is known as robustness bounds.

However, even with these techniques, one is still not yet ready to handle real experimental data. The reason is that self-testing operates under the assumption of what is known as the no-signalling condition, which raw experimental data does not fulfill (almost all of the time). Therefore, one first needs to perform a projection of the raw data into the set of correlations that *do* obey the no-signalling condition, obtaining a projected probability point which then can be used to determine the lower bound onfidelity. This process is known as Regularisation[4].

This report will first present in detail well-established ideas of self-testing and robustness curves. Then, the idea and method of regularisation will be discussed. Following this, these tools will be applied to data obtained from a simulator which simulates data for the CHSH scenario, and also from experimental data obtained from IBM's Q experience. Lastly, self-testing in the double CHSH scenario will be briefly discussed.

2 Preliminaries

2.1 Basic Notation

Throughout this report, the following scenario will be considered: Two parties (Alice and Bob) both possess a box into which they input settings, to which the box responds by giving an output. The inputs (settings) are denoted by x and y, while the outputs are denoted by a and b for Alice and Bob respectively. Also, the no-signalling condition is assumed to always hold. This means that both parties are space-like separated so that no classical communication takes place between them.

Besides the no-signalling assumption, nothing else is assumed about the boxes; in particular, no assumptions are made on the inner workings or mechanisms that may lie within the boxes. Hence, the boxes can in fact be viewed effectively as two blackboxes which simply receive inputs and give outputs. This setup is depicted in figure 1 below:

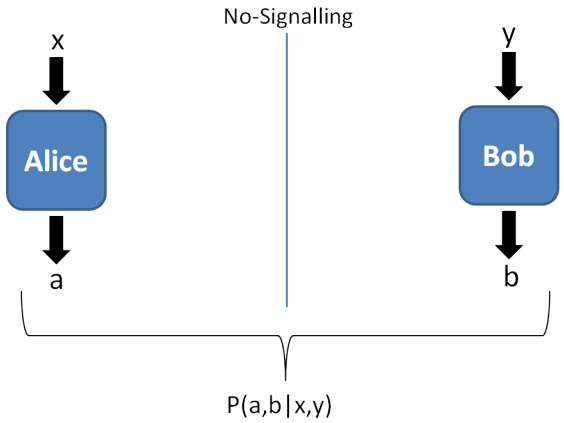

Figure 1: Setup for Alice and Bob

Here, both Alice and Bob collect data by giving their boxes inputs x, y, and recording the corresponding outputs a, b. They each perform many such runs and record the data for each run individually as (a, x) for Alice and (b, y) for Bob. They then come together to combine their data and end up with something of the form (a, b, x, y) for each run. With this data, they can then estimate the joint probabilities (correlations), denoted by $P(a, b|x, y)$.

As a concrete example, if both the outputs and inputs are binary, $x, y \in \{0, 1\}$, $a, b \in \{-1, 1\}$ as in the CHSH case (which will be further examined), the correlations $P(a, b|x, y)$ can be written as a vector with 16 entries as follows:

$$\begin{pmatrix} P(++|00) \\ P(+-|00) \\ P(-+|00) \\ P(--|00) \\ \vdots \\ P(--|11) \end{pmatrix}$$

2.2 No-Signalling Condition

The no-signalling condition, as mentioned briefly in the previous section, are the following set of constraints:

$$P(a|x) = \sum_b P(a, b|x, y) = \sum_b P(a, b|x, y') \tag{1}$$

$$P(b|y) = \sum_a P(a, b|x, y) = \sum_a P(a, b|x', y) \tag{2}$$

This means the following: The marginal probability that Alice obtains outcome a, given her input setting x, is independent of whatever setting Bob chooses. This is because Alice and Bob cannot communicate with one another, and so Bob's setting should not affect outcome of Alice's measurement. The same reasoning naturally also applies to Bob.

A final note here is that this is not the most general scenario one can have. In general, one may consider situations with more than two parties. Nevertheles, the joint probabilities are obtained in the same way, demanding the corresponding no-signalling conditions to hold. Also, the number of settings and possible outcomes may also vary, depending on scenario under consideration. That being said, this report will focus only on the case of two parties, which can be adequately described with the notation presented thus far.

3 Self-Testing

3.1 An Analogy: Fingerprinting

Self-testing is in a way, similar to fingerprinting, in the sense that given a fingerprint, one can identify the one and only person it belongs to. In self-testing, this "fingerprint" comes in the form of observed correlations obtained from experimental data. Given that one observes *some* correlations, one can identify uniquely both the state Alice and Bob share, as well as the measurements they must have made on the state, which gave rise to those correlations.

Moreover, just as how a person has 10 different fingerprints (one for each finger), each state can also have multiple "fingerprints". In other words, each state can have a few signature correlations, all of which self-test the same state and measurements, but yet are not equivalent to each other. Therefore, observation of any one of those correlations (criteria) allows one to identify uniquely the state and the measurements performed on it.

However, due to the quantum nature of self-testing, the reality of the situation is slightly different from the fingerprint analogy. In fingerprinting, one is able to identify the one and only person it belongs to, whereas in self-testing, there are in fact various possible quantum realisations (states and measurements:$|\psi\rangle, \Pi_a^x, \Pi_b^y$) that can give rise to a set of correlations known to self-test a specific state $|\bar{\psi}\rangle$. The key point here, however, is that all these possible states and measurements are in fact equivalent to one another, and so can be mapped by what is known as an isometry[1, 5] to the specific state and measurements the correlations are known to self-test ($|\bar{\psi}\rangle, \{\bar{\Pi}_a^x, \bar{\Pi}_b^y\}$). Note that the ideal state and measurements that are being tested will be denoted by a bar above.

3.2 Self Testing: The main idea

In this section, the idea of self-testing will be presented more concretely. Self-testing in essence refers to the fact that the observation of *some* correlations $P(a, b|x, y)$, as established in section 2.1, allows one to identify uniquely a state $|\bar{\psi}\rangle$ and suitable measurements on the state $\{\bar{\Pi}_a^x, \bar{\Pi}_b^y\}$ that are compatible with the observed $P(a, b|x, y)$. This is captured by the following expression:

$$P(a,b|x,y) = \langle\bar{\psi}|\,\bar{\Pi}_a^x \otimes \bar{\Pi}_b^y\,|\bar{\psi}\rangle \tag{3}$$

In other words, for *some* observed correlations $P(a,b|x,y)$ obtained by Alice and Bob, one can conclusively infer the state $|\bar{\psi}\rangle$ that Alice and Bob *must* have shared. On top of that, one can determine the measurements $\{\bar{\Pi}_a^x, \bar{\Pi}_b^y\}$ Alice and Bob were making on the state when they chose their settings x and y.

However, as metioned in section 3.1, saying that one can determine the state uniquely *does not* mean that there exists only one possible state which gives us the observed $P(a,b|x,y)$. To rephrase, given some observed correlations $P(a,b|x,y)$ known to self-test a particular state, it does not necessarily mean that Alice and Bob indeed shared this state. However, the state shared and measurements performed *are equivalent* to the state and measurements $(|\bar{\psi}\rangle, \{\bar{\Pi}_a^x, \bar{\Pi}_b^y\})$ the correlations are known to self-test, up to a local isometry. Briefly, this means that the state (and measurements) in the lab $|\psi\rangle$ differs from the state the correlations are known to self-test $|\bar{\psi}\rangle$ up to local unitaries or addition of irrelevant degrees of freedom. This will be further elaborated on in section 3.4, where the formal definition of Self-Testing is presented.

Lastly, one should note that not just any observed $P(a,b|x,y)$ obtained from an experiment allows one to self-test some state. It is possible (in fact more likely) that looking at just any $P(a,b|x,y)$ does not allow one to identify any state. It is only *some very specific* correlations that allow one to self-test certain states.

3.3 Device-Independence and its implications

Before proceeding further, Device-Independence, an intricacy of the ideas presented so far will be briefly discussed. The fact that one can draw conclusions about Alice's and Bob's boxes by looking at *only* the $P(a,b|x,y)$ (and nothing else) is characteristic of what is known as Device-Independence. More succinctly, we say that self-testing is device-independent.

The origin of the term is easy to understand. Device-independence refers to the idea that one can be completely ignorant of the contents of Alice's and Bob's boxes, but still be able to obtain information about the state (and measurements) that they must have shared. Therefore conclusions are drawn by

only looking at the inputs and outputs, independent of whatever may be contained in the boxes, hence the term device-independence. Self-testing and it's Device-Independent nature in fact has practical applications in many quantum information protocols, one of which is state certification which will now be briefly explained.

Quantum state certification is, as the name suggests, certifying that one is in possession of some desired quantum state. Self-testing allows one to perform such a certification since the mere observation of correlations allows one to make conclusions on the state. One can therefore verify if a state prepared in the lab is indeed the desired state just by checking if the $P(a, b|x, y)$ obtained is characteristic of the target state. In fact, as will be explained later, one can actually quantify, and provide a meaningful measure of how "close" a state is to the target state by using the tools of self-testing and some other ideas.

One of state certification is in quantum cryptography. In quantum key distribution, it is necessary that Alice and Bob share an entangled state in order to ensure they both have access to a secure key. In order to ensure that the state they share is indeed the desired entangled state, one can feed the boxes with inputs and obtain the corresponding outputs and compute the correlations $P(a, b|x, y)$. With that information, one can then determine if the state is indeed the target state (or at least sufficiently "close" to the target state), and therefore certify the entanglement and security of the protocol.

3.4 The formal definition of Self-testing

Formally, Self-testing is presented as the following[1, 5]: For every possible quantum realisation $(|\psi\rangle, \Pi_a^x, \Pi_b^y\})$ compatible with the correlations $P(a, b|x, y)$, there exists a local isometry $\Phi = \Phi_A \otimes \Phi_B$ such that:

$$\Phi |\psi\rangle = |\bar{\psi}\rangle_{A'B'} \otimes |junk\rangle_{AB} \tag{4}$$

$$\Phi(\Pi_a^x \otimes \Pi_b^y |\psi\rangle) = (\bar{\Pi}_a^x \otimes \bar{\Pi}_b^y |\bar{\psi}\rangle)_{A'B'} \otimes |junk\rangle_{AB} \tag{5}$$

Here, A and B denote the systems of Alice's and Bob's boxes, while A' and B' are two ancillary qubits. This means that for every possible state $|\psi\rangle$ and measurements $\{\Pi_a^x, \Pi_b^y\}$ that gives the correlations $P(a, b|x, y)$, one can

find a local isometry that maps the state $|\psi\rangle$ to the unique state $|\bar{\psi}\rangle$, as well as the measurements $\{\Pi_a^x, \Pi_b^y\}$ to the appropriate measurements $\{\bar{\Pi}_a^x, \bar{\Pi}_b^y\}$ on the unique state $|\bar{\psi}\rangle$. Therefore, all the possible states $|\psi\rangle$ that give those correlations are equivalent to the unique state $|\bar{\psi}\rangle$ up to some local isometry Φ. The details of the implementation of such an isometry will be elaborated on in section 5.1, where it is applied together with some other tools that will be discussed later in order to facilitate a smoother flow of ideas.

It should be noted that an isometry is only a virtual protocol, a theoretical procedure. Thus, it is not actually carried out in the lab when one implements self-testing. All that is required in the lab is to query the boxes with the inputs x, y and obtain the outcomes a, b which allow one to estimate the probabilities $P(a, b|x, y)$, which is sufficient for one to perform self-testing.

3.5 An example: The CHSH criteria for Self-testing

An example of Self-testing will now be presented: the CHSH criterion, where the value of the CHSH expression, derived by Clauser, Horne, Shimony, and Holt[2, 11] is used to self-test the singlet state. In this scenario, Alice and Bob both have two settings to choose from, $x, y \in \{0, 1\}$. For each setting, the boxes give one of two outputs, $a, b \in \{-1, +1\}$. The CHSH is given by the following expression:

$$CHSH = \langle A_0 B_0 \rangle + \langle A_0 B_1 \rangle + \langle A_1 B_0 \rangle - \langle A_1 B_1 \rangle \tag{6}$$

Here, $\langle A_x B_y \rangle$ denotes the expectation value of the product of Alice's outcome given she chose setting x, and Bob's outcome given he chose setting y. This CHSH expression is a well known Bell-Inequality, which must satisfy $CHSH \leq 2$ if local hidden variable theories (such as the one proposed by Einstein, Podolsky and Roden) are true[3]. However, this inequality can be violated by quantum mechanics. More impressive is the fact that the violation is exactly as predicted by quantum mechanics. Using quantum mechanical ideas, one can show that the maximum value [3, 11]that it can take is $CHSH = 2\sqrt{2}$.

Remarkably, it has also been discovered that the CHSH value can be used in self-testing. In particular, the observation of $CHSH = 2\sqrt{2}$ self-tests the maximally entangled state of two qubits $|\Phi^+\rangle = \frac{1}{\sqrt{2}}\big(|00\rangle + |11\rangle\big)$, which will be referred to as the singlet state in this report. This means that given some

observed correlations $P(a,b|x,y)$, we can calculate the value of the CHSH expression, and *if and only if* we find that $CHSH = 2\sqrt{2}$, we can conclude that the state is the singlet state. To draw a link to the analogy presented in section 3.1, one can think of $CHSH = 2\sqrt{2}$ as one of the "fingerprints" of the singlet state.

3.6 Another criterion for self-testing of the singlet: the Mayers-Yao Statistics

As mentioned earlier, there are many different criteria ("fingerprints") that allow one to self-test the singlet state. Observation of $CHSH = 2\sqrt{2}$ is one of them, and here, another such criteria will be discussed; The Mayers-Yao criterion [3].

In this scenario, instead of having 2 settings for each party, there are 2 settings on Alice's box, and 3 settings on Bob's box. The outputs remain binary as in the CHSH case. The settings on the boxes will be denoted by $\{X_A, Z_A; X_B, Z_B, D_B\}$, where the subscript indicates the box which the measurement is performed on.

If one observes the following correlations:

$$\langle\Psi| Z_A Z_B |\Psi\rangle = \langle\Psi| X_A X_B |\Psi\rangle = 1 \tag{7}$$

$$\langle\Psi| X_A Z_B |\Psi\rangle = \langle\Psi| Z_A X_B |\Psi\rangle = 0 \tag{8}$$

$$\langle\Psi| Z_A D_B |\Psi\rangle = \langle\Psi| X_A D_B |\Psi\rangle = \frac{1}{\sqrt{2}} \tag{9}$$

One can show[3] that the state $|\Psi\rangle$ must be equivalent to the state $|\Phi^+\rangle$, and that the measurements are effectively the corresponding pauli matrices
$(Z \to \sigma_z, X \to \sigma_x)$, where $D \to \frac{1}{\sqrt{2}}(\sigma_z + \sigma_x)$.

The Mayers-Yao Criterion here is different from the CHSH one, although both self-test the same singlet state. Therefore, both of these can be seen as different "fingerprints" of the singlet state. Additionally, for the case of two binary measurements in a bi-partite scenario, it has been shown that all the possible criterion for self-testing can be characterised[8].

4 Applying Self-Testing

4.1 Non-ideal Correlations

So far, the idea of Self-Testing and it's possible applications have been discussed in some detail. However, it should be noted that self-testing in principle only works in an ideal situation, where the correlations observed are perfect and exact. For instance, in the CHSH case, one has to observe $CHSH = 2\sqrt{2}$ *exactly*, in order to conclude that the state is indeed the singlet state.

However, in the lab, one will observe $CHSH = 2\sqrt{2} - \epsilon$, where ϵ represents some error arising from inevitable experimental imperfections and statistical fluctuations. The question then arises: what then can be inferred about the state from the data? One therefore requires some method which quantifies the closeness of the state one has in the lab (from which data is collected) to the ideal state is needed. It turns out that a tool known as robustness bounds does exactly that.

4.2 Fidelity and Robustness bounds

Firstly, given some data, one can calculate a quantity known as the fidelity, which describes the overlap between a state and the state one wishes to self-test(the ideal state). The expression of the fidelity is as follows[5]:

$$F = Tr(\rho_{ideal}\rho_{A'B'}) \tag{10}$$

Here, ρ_{ideal} is the density matrix of the state we wish to self-test (for the singlet state, $\rho_{ideal} = |\Phi^+\rangle \langle\Phi^+|$) and $\rho_{A'B'}$ is the density matrix of the ancillas A' and B', after the isometry (as mentioned in Section 3.4) has been applied. The expression of $\rho_{A'B'}$ contains information from data one obtains in the lab, together with a bunch of variables, which will then be varied by means of a computer program to minimise the objective function, F. The result of this minimisation returns the lowest possible fidelity with the state, given some data from which one estimates the probabilities $P(a, b|x, y)$. This will be explicitly demonstrated in section 5.

The intuition here is that given some CHSH value, $CHSH = 2\sqrt{2} - \epsilon$, it is possible that there exist many states $|\psi\rangle$ which gives that particular value, each

of which have a different fidelity with the target state $|\Phi^+\rangle$. Since no assumptions are made on the contents of the boxes, and only the statistics obtained are considered, the lowest fidelity is taken. By doing so, one obtains a lower bound on the fidelity which is the "worst-case scenario". Therefore, it could be that the state has a higher fidelity than this minimum fidelity F_{min}, but one can be sure that the fidelity is at least F_{min}. In essence, given observed correlations from experimental data, this approach allows one to find the minimum fidelity with the ideal state F_{min}, and be sure that the actual fidelity, F, is such that $F \geq F_{min}$.

With this in mind, one can plot a graph of fidelity against ϵ, which shows how the minimum fidelity changes as the deviation from the target state becomes larger. Such a graph is known as a robustness curve and it is shown below:

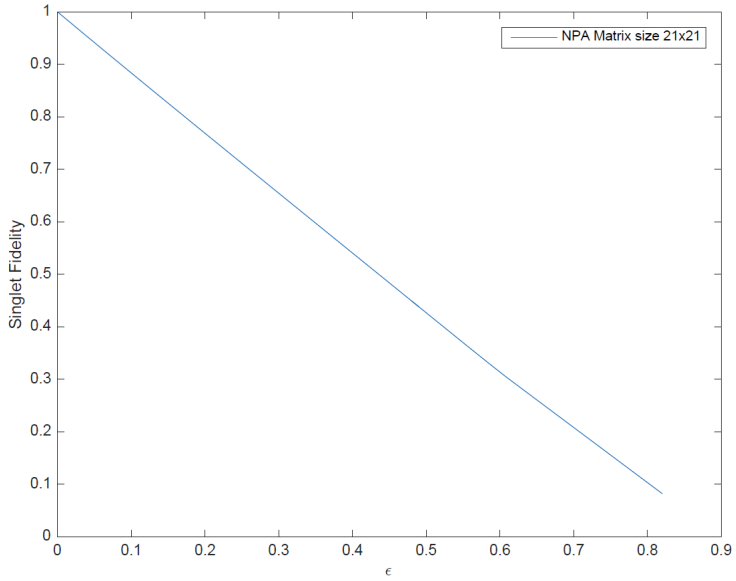

Figure 2: Robustness Curve for CHSH criterion

As seen here, when ϵ is 0, one has the perfect data, giving a fidelity of 1, which is self-testing in the ideal case where the ideal correlations are obtained. As ϵ increases, the fidelity falls, which is expected as the deviation away from the ideal state increases. This therefore enables one to quantify exactly how "close" a state is to the ideal state. Note that a trivial bound of the fidelity is

$F = 0.5$, as that corresponds to the maximally mixed state. As such, $F = 0.5$ is the worst fidelity one can obtain, and gives no information on the state. Note that while the graph in figure 2 drops below $F = 0.5$, all points with $F < 0.5$ can be treated as having a fidelity of $F = 0.5$, corresponding to the maximally mixed state.

Given that there are different criteria to self-test a state, as mentioned in sections 3.5 and 3.6, one obtains different lower bounds on the fidelity by using the different criteria. Of course, if the objective here is to self-test the singlet, one ought to pick the criterion that gives the highest lowest bound on the fidelity.

Also, it is important to keep in mind that it is possible for different $P(a, b|x, y)$ to give the same CHSH value (where $\epsilon \neq 0$), and each of those $P(a, b|x, y)$ might each give a different fidelity with the singlet. Therefore, in figure 2, the fidelity here is the *minimum* possible one out of all the $P(a, b|x, y)$ that gives the same CHSH value. In an experiment however, one has access not only to the CHSH value, but also the full statistics $P(a, b|x, y)$. Using these statistics to directly compute the fidelity can actually give one a better lower bound (as demonstrated later in section 6.6.)

4.3 Regularisation

So far, self-testing and its practical application using robustness curves has been discussed in some detail. At this point, it may be tempting to think one is ready to implement this on actual data from the lab, since it seems that one already has all the necessary tools.

However, that is not the case. The procedure that has been outlined so far is based on the assumption that the correlations $P(a, b|x, y)$ obtained are in the quantum set of correlations, Q, which *must* satisfy the no-signalling condition as mentioned in section 2.2. There is, however, absolutely no guarantee that this holds for data that is obtained from the lab . In fact, most of the time, the no-signalling conditions *do not hold* for raw experimental data.

Therefore, before the raw data is analysed, one must first make sure that it is indeed no-signalling. To do this, one has to project the point into a superset relaxation of the quantum set of probabilities, Q_l. One way of performing this

projection[4] is to find the point that lies in Q_l which minimises the two-norm from the raw experimental data point:

$$\vec{P}_{NQA_2}(\vec{P}_{exp}) = \text{argmin}_{\vec{P}\in Q_l} \|\vec{P}_{exp} - \vec{P}\|_2 \tag{11}$$

Here, one attempts to find the point within Q_l that minimises the "distance" from the experimental point $\vec{P}_{exp}$. This projected point, being in the set of Q_l, will necessarily satisfy the No-Signalling conditions. Note that the reason a superset relaxation of the quantum set is used is that the quantum set is not fully characterised[6]. Here, the subscript NQA_2 stands for the "Nearest Quantum Approximation" and 2 stands for the 2-norm. Once this projection is complete, one obtains a regularised point, which only then can be legitimately used in for further analysis to obtain the fidelity. This process can be visualised as illustrated in the following diagram:

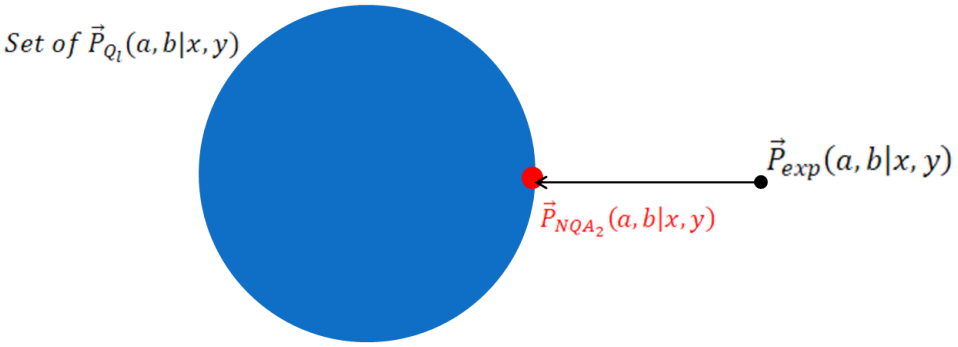

Figure 3: Projection of raw probability point $\vec{P}_{exp}(a,b|x,y)$ into the set Q_l

5 Self-Testing in detail: CHSH

In this section, the details regarding the procedures of how one can implement self-testing will be discussed. Ultimately, the aim here is to provide a valid lower bound for the fidelity of a state, given some experimental data from the lab. Ideas that were discussed earlier will now be presented more concretely, and the details will be thoroughly explained.

5.1 The Isometry

The ideal case will first be considered. Given a state shared by Alice and Bob, $|\bar{\psi}\rangle$, one needs an isometry that maps this state into the ancilla systems A' and B'. Mathematically, this is captured by the following:

$$\Phi \, |\bar{\psi}\rangle_{AB} = |\bar{\psi}\rangle_{A'B'} \otimes |junk\rangle_{AB} \tag{12}$$

An explicit example of such an isometry is the following[3]:

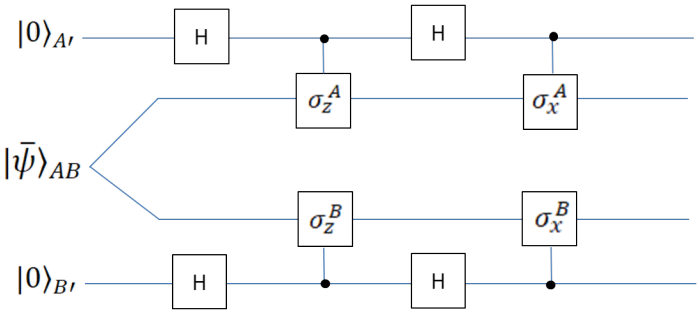

Figure 4: Isometry that maps the singlet state into the ancilla qubits

This is the equivalent of what is known as a SWAP isometry[5]. The top and bottom lines represent the ancilla qubits, systems denoted by A' and B'. H is the hadamard gate which acts as follows: $H\,|0\rangle = \frac{|0\rangle+|1\rangle}{\sqrt{2}}$, $H\,|1\rangle = \frac{|0\rangle-|1\rangle}{\sqrt{2}}$. The σ_i's here are the usual sigma matrices, with the superscripts denoting which qubit they act on.

This isometry here actually acts as a swap (hence the name) between the ancilla qubits and the state shared by Alice and Bob: $|\bar{\psi}\rangle_{AB}\,|00\rangle_{A'B'} \rightarrow |00\rangle_{AB}\,|\bar{\psi}\rangle_{A'B'}$. This mapping will now be demonstrated using the following state (for convenience): $|\bar{\psi}\rangle = |\Phi^+\rangle = \frac{1}{\sqrt{2}}\big(\,|00\rangle + |11\rangle\,\big)$

First, the Hadamard gates act on the ancilla systems which gives the following:

$$\begin{aligned}\frac{1}{\sqrt{2}}\big(\,|00\rangle+|11\rangle\,\big)_{AB}\,|00\rangle_{A'B'} \rightarrow &\frac{1}{\sqrt{2}}\big(\,|00\rangle+|11\rangle\,\big)_{AB}\Big(\frac{|0\rangle+|1\rangle}{\sqrt{2}}\Big)_{A'}\Big(\frac{|0\rangle+|1\rangle}{\sqrt{2}}\Big)_{B'}\\ &=\frac{1}{2\sqrt{2}}\big(\,|00\rangle_{AB}\,\big)\big(\,|00\rangle+|01\rangle+|10\rangle+|11\rangle\,\big)_{A'B'}\\ &+\big(\,|11\rangle_{AB}\,\big)\big(\,|00\rangle+|01\rangle+|10\rangle+|11\rangle\,\big)_{A'B'}\end{aligned} \tag{13}$$

From here on, the subscripts indicating the system(A and B) and the ancillas (A' and B') will be dropped. It shall be understood that the first two digits in any ket corresponds to A and B, while the last two correspond to A' and B' respectively.

The ancillas now act as what is known as a control qubit. In this case, the operation σ_z is performed on the Alice's/Bob's qubit only if the control qubit(ancilla) is in the state $|1\rangle$. If the control qubit is in the state $|0\rangle$, no operation is performed (or equivalently the identity operation). With this one obtains the following, bearing in mind that $\sigma_z\,|0\rangle=|0\rangle$, $\sigma_z\,|1\rangle=-\,|1\rangle$:

$$\begin{aligned}\frac{1}{2\sqrt{2}}\big(\,&|0000\rangle+|0001\rangle+|0010\rangle+|0011\rangle\\ &+|1100\rangle-|1101\rangle-|1110\rangle+|1111\rangle\,\big)\end{aligned} \tag{14}$$

After applying the next two hadamard gates to the ancillas in an identical fashion as before and doing some simplification, the following is obtained:

$$\frac{1}{\sqrt{2}}\big(\,|0000\rangle+|1111\rangle\,\big) \tag{15}$$

Finally, upon applying the last two σ_x matrices, one obtains :

$$\begin{aligned}\frac{1}{\sqrt{2}}\big(\,|0000\rangle+|0011\rangle\,\big)&=\frac{1}{\sqrt{2}}\,|00\rangle_{AB}\,\big(\,|00\rangle+|11\rangle\,\big)_{A'B'}\\ &=|00\rangle_{AB}\,|\bar{\psi}\rangle_{A'B'}\end{aligned} \tag{16}$$

Therefore, with this isometry, the singlet state that Alice and Bob share is swapped into the ancilla systems. This isometry here is in general valid for any starting state, in the sense that it swaps whatever state one begins with into the ancilla systems.

5.2 Ideal State, Measurements, and other details

The CHSH criterion will be used to self-test the singlet. The ideal state shall be written as the following[5]:

$$|\bar{\psi}\rangle = \cos\frac{\pi}{8}|\Phi^-\rangle + \sin\frac{\pi}{8}|\Psi^+\rangle \tag{17}$$

Here, $|\Phi^-\rangle = \frac{1}{\sqrt{2}}(|00\rangle - |11\rangle)$ and $|\Psi^+\rangle = \frac{1}{\sqrt{2}}(|01\rangle + |10\rangle)$. Note that as this is a superposition of two maximally entangled states, it is therefore, still equivalent(up to local unitaries) to the singlet state. The measurements that we want to self-test are then $\bar{A}_0 = \sigma_z, \bar{A}_1 = \sigma_x, \bar{B}_0 = \sigma_z, \bar{B}_1 = \sigma_x$. With this state and the corresponding pauli matrices as the measurements, one can calculate the value of the $CHSH$ expression and obtain $CHSH = 2\sqrt{2}$, the maximal violation. This will now be demonstrated:

$$\begin{aligned}\left\langle \bar{A}_0\bar{B}_0 \right\rangle =& \langle\bar{\psi}|\, \bar{A}_0\bar{B}_0\, |\bar{\psi}\rangle \\ =& c^2 \langle\Phi^-|\, \sigma_z\otimes\sigma_z\, |\Phi^-\rangle + cs\, \langle\Psi^+|\, \sigma_z\otimes\sigma_z\, |\Phi^-\rangle \\ &+ cs\, \langle\Phi^-|\, \sigma_z\otimes\sigma_z\, |\Psi^+\rangle + s^2\, \langle\Psi^+|\, \sigma_z\otimes\sigma_z\, |\Psi^+\rangle\end{aligned}$$

Here, $c = \cos\frac{\pi}{8}$ and $s = \sin\frac{\pi}{8}$. Since $|\Phi^-\rangle = \frac{1}{\sqrt{2}}(|00\rangle - |11\rangle)$ and $|\Psi^+\rangle = \frac{1}{\sqrt{2}}(|01\rangle + |10\rangle)$,

$$\begin{aligned}\sigma_z\otimes\sigma_z\, |\Phi^-\rangle =& |\Phi^-\rangle \\ \sigma_z\otimes\sigma_z\, |\Psi^+\rangle =& -|\Psi^+\rangle\end{aligned}$$

Using the property that the bell states are orthogonal ($\langle\Phi^-|\Psi^+\rangle = 0$), one obtains:

$$\begin{aligned}\left\langle \bar{A}_0\bar{B}_0 \right\rangle =& \cos^2\frac{\pi}{8} + \sin^2\frac{\pi}{8} \\ =& \cos(\frac{\pi}{4}) \\ =& \frac{1}{\sqrt{2}}\end{aligned}$$

Repeating the same calculation for the other combinations of settings one obtains the following:

$$\left\langle \bar{A}_x \bar{B}_y \right\rangle = \frac{1}{\sqrt{2}}(-1)^{xy} \implies CHSH = 2\sqrt{2} \tag{18}$$

Also, since experimental data comes in the form $P(a,b|x,y)$, knowing the conversion from $P(a,b|x,y)$ to the quantities $\langle A_x \rangle, \langle B_y \rangle$ and $\langle A_x B_y \rangle$ is convenient:

$$\begin{aligned}
\langle A_x \rangle =& (+1)P(a=+1|x) + (-1)P(a=-1|x) \\
=& P(++|x,y) + P(+-|x,y) - P(-+|x,y) - P(--|x,y) \\
\\
\langle B_y \rangle =& (+1)P(b=+1|y) + (-1)P(b=-1|y) \\
=& P(++|x,y) + P(-+|x,y) - P(+-|x,y) - P(--|x,y) \\
\\
\langle A_x B_y \rangle =& P(a=b) - P(a\neq b) \\
=& P(++|x,y) + P(--|x,y) - P(+-|x,y) - P(-+|x,y)
\end{aligned} \tag{19}$$

$P(a,b|x,y)$ can also be expressed in terms of $\langle A_x \rangle, \langle B_y \rangle$ and $\langle A_x B_y \rangle$:

$$\begin{aligned}
A_x =& \Pi^x_{+1} - \Pi^x_{-1} \\
B_y =& \Pi^y_{+1} - \Pi^y_{-1}
\end{aligned}$$

Π^x_a represents the projector given the outcome a and input setting x. Since the projectors sum to identity, $\Pi^x_{+1} + \Pi^x_{-1} = \mathbb{1}$, one can express them in terms of the operators A_x and B_y as follows:

$$\begin{aligned}
\Pi^x_a =& \frac{\mathbb{1} + aA_x}{2} \\
\Pi^y_b =& \frac{\mathbb{1} + bB_y}{2}
\end{aligned}$$

Finally, one obtains the following expression for $P(a,b|x,y)$:

$$
\begin{aligned}
P(a,b|x,y) &= \langle\psi|\, \Pi_a^x \otimes \Pi_b^y \,|\psi\rangle \\
&= \langle\psi|\, \frac{\mathbb{1} + aA_x}{2} \otimes \frac{\mathbb{1} + bB_y}{2} \,|\psi\rangle \\
&= \frac{1}{4}(1 + a\,\langle A_x\rangle + b\,\langle B_y\rangle + ab\,\langle A_x B_y\rangle)
\end{aligned} \tag{20}
$$

5.3 The Fidelity

The derivation of an expression for the fidelity with the singlet state will now be demonstrated. First, the exact same isometry as in section 5.1 is applied, but now without making any assumption on the state that Alice and Bob share, and also none on the measurement settings. The reasoning is here is that if one is promised that Alice and Bob share a singlet state and that the measurements are indeed the pauli matrices as claimed, we should be able to run the exact same setup and end up with the singlet being swapped into the ancillas.

Removing the assumptions on the state and measurements, one then has the state $|\psi\rangle_{AB}$ shared by Alice and Bob (instead of $|\bar{\psi}\rangle$), and measurements that will now be denoted by A_x, B_y (instead of σ_i's). Therefore, the state and measurements in the previous isometry are replaced with the new state and measurements which gives the following:

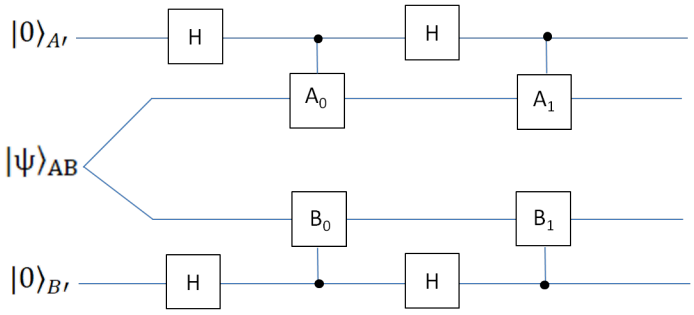

Figure 5: Isometry with sigma matrices replaced with actual measurements

The state obtained in the two ancillas A' and B' then needs to be computed, which will be denoted by the density matrix $\rho_{A'B'}$. However, to do that, the final state $\rho_{ABA'B'}$ after the isometry has been applied will first need to be calculated: $\rho_{ABA'B'} = [\Phi\,|\psi\rangle\,|00\rangle][\Phi\,|\psi\rangle\,|00\rangle]^\dagger$. Proceeding analogously to the

calculation in section 5.1 and noting that A_x and B_y commute, one obtains the following:

$$\begin{aligned}\Phi\left|\psi\right\rangle\left|00\right\rangle =&\frac{1}{4}(\mathbb{1}+A_0)(\mathbb{1}+B_0)\left|\psi\right\rangle\left|00\right\rangle+\\&A_1B_1(\mathbb{1}-A_0)(\mathbb{1}-B_0)\left|\psi\right\rangle\left|11\right\rangle+\\&B_1(\mathbb{1}+A_0)(\mathbb{1}-B_0)\left|\psi\right\rangle\left|01\right\rangle+\\&A_1(\mathbb{1}-A_0)(\mathbb{1}+B_0)\left|\psi\right\rangle\left|10\right\rangle\end{aligned} \tag{21}$$

$$\begin{aligned}\left[\Phi\left|\psi\right\rangle\left|00\right\rangle\right]^\dagger =&\frac{1}{4}\left\langle\psi\right|\left\langle 00\right|(\mathbb{1}+B_0)(\mathbb{1}+A_0)+\\&\left\langle\psi\right|\left\langle 11\right|(\mathbb{1}-B_0)(\mathbb{1}-A_0)B_1A_1+\\&\left\langle\psi\right|\left\langle 01\right|(\mathbb{1}-B_0)(\mathbb{1}+A_0)B_1+\\&\left\langle\psi\right|\left\langle 10\right|(\mathbb{1}+B_0)(\mathbb{1}-A_0)A_1\end{aligned} \tag{22}$$

Multiplying (21) and (22), the state $\rho_{ABA'B'}$ is obtained. This can be represented as a matrix containing 16 terms, where the first term is the following:

$$(\rho_{ABA'B'})_{11}=\frac{1}{16}(\mathbb{1}+A_0)(\mathbb{1}+B_0)\left|\psi\right\rangle\left\langle\psi\right|\left|00\right\rangle\left\langle 00\right|(\mathbb{1}+B_0)(\mathbb{1}+A_0) \tag{23}$$

The other 15 terms then follow analogously. Next, only the state of the ancilla systems is desired, the partial trace is taken: $\rho_{A'B'}=Tr_{AB}(\rho_{ABA'B'})$. For the first term, noting that $A_x^2=B_y^2=\mathbb{1}$ one obtains:

$$\begin{aligned}(\rho_{A'B'})_{11} =&Tr_{AB}((\rho_{ABA'B'})_{11})\\=&\frac{1}{16}\left\langle\psi\right|(\mathbb{1}+B_0)(\mathbb{1}+A_0)(\mathbb{1}+A_0)(\mathbb{1}+B_0)\left|\psi\right\rangle\left|00\right\rangle\left\langle 00\right|\\=&\frac{1}{16}\left\langle\psi\right|(\mathbb{1}+A_0)^2(\mathbb{1}+B_0)^2\left|\psi\right\rangle\left|00\right\rangle\left\langle 00\right|\\=&\frac{1}{4}\left\langle\psi\right|(\mathbb{1}+A_0+B_0+A_0B_0)\left|\psi\right\rangle\left|00\right\rangle\left\langle 00\right|\end{aligned} \tag{24}$$

Proceeding in the same way, one then obtains all the other terms $(\rho_{A'B'})_{ij}$.

Next, the fidelity will be calculated. The expression for the fidelity is $F=Tr(\rho_{ideal}\rho_{A'B'})$. It is therefore necessary to first work out the ideal state $\rho_{ideal}=$

$|\bar{\psi}\rangle\langle\bar{\psi}|$, where $|\bar{\psi}\rangle = \cos\frac{\pi}{8}|\Phi^-\rangle + \sin\frac{\pi}{8}|\Psi^+\rangle$ as mentioned in equation (17):

$$\begin{aligned}|\bar{\psi}\rangle =& \cos\frac{\pi}{8}|\Phi^-\rangle + \sin\frac{\pi}{8}|\Psi^+\rangle \\ =& \frac{1}{\sqrt{2}}[c|00\rangle + s|01\rangle + s|10\rangle - c|11\rangle]\end{aligned}$$

The density matrix is then

$$\begin{aligned}\rho_{ideal} = \frac{1}{2}[&c^2|00\rangle\langle 00| + cs|00\rangle\langle 01| + cs|00\rangle\langle 10| - c^2|00\rangle\langle 11| \\ &+cs|01\rangle\langle 00| + s^2|01\rangle\langle 01| + s^2|01\rangle\langle 10| - cs|01\rangle\langle 11| \\ &+cs|10\rangle\langle 00| + s^2|10\rangle\langle 01| + s^2|10\rangle\langle 10| - cs|10\rangle\langle 11| \\ &-c^2|11\rangle\langle 00| - cs|11\rangle\langle 01| - cs|11\rangle\langle 10| + c^2|11\rangle\langle 11|]\end{aligned}$$

Here, c and s stand for $\cos\frac{\pi}{8}$ and $\sin\frac{\pi}{8}$ respectively. Note that ρ_{ideal} can also be cast into a 16 by 16 matrix with elements $(\rho_{ideal})_{ij}$, with the first element being $(\rho_{ideal})_{11} = \frac{1}{2}\cos^2\frac{\pi}{8}$. To find the fidelity, the state ρ_{ideal} is then multiplied to $\rho_{A'B'}$ since $F = Tr(\rho_{ideal}\rho_{A'B'})$. Also, as the trace is taken, one only needs the diagonal terms. Therefore,

$$\begin{aligned}F =& \sum_{i=1}^{4}(\rho_{ideal}\rho_{A'B'})_{ii} \\ =& \sum_{i=1}^{4}\left(\sum_{j=1}^{4}(\rho_{ideal})_{ij}(\rho_{A'B'})_{ji}\right)\end{aligned} \tag{25}$$

Inserting all the terms and taking the sum as in equation (25), one finally obtains the following expression for the fidelity:

$$\begin{aligned}F =& \frac{1}{4} + \frac{1}{4\sqrt{2}}\langle A_0B_0 + A_0B_1 + A_1B_0 - A_1B_1\rangle \\ &- \frac{1}{16}\langle A_0A_1B_0B_1 - A_0A_1B_1B_0 - A_1A_0B_0B_1 + A_1A_0B_1B_0\rangle \\ &+ \frac{1}{16\sqrt{2}}\langle 3A_1B_1 - 2A_0B_1 - 2A_1B_0 + A_0A_1A_0B_1 - 2A_0A_1A_0B_0 \\ &+ A_1B_0B_1B_0 - 2A_0B_0B_1B_0 - A_0A_1A_0B_0B_1B_0\rangle\end{aligned} \tag{26}$$

5.4 The Moment Matrix and Semi-Definite Programs (SDP)

Looking the expression of the fidelity, terms like $\langle A_0 A_1 B_0 B_1 \rangle$ appear, which represent the expectation values of the outcomes of two successive measurements (A_0 and A_1) on Alice's side and the same for Bob (B_0 and B_1) for a single run of the experiment. However, in one run, only one measurement is made per side, one for Alice and one for Bob. Therefore, one can only obtain values of the marginals, $\langle A_x \rangle \,\&\, \langle B_y \rangle$, and the values of what are known as the correlators, $\langle A_x B_y \rangle$, but not values of terms like $\langle A_0 A_1 B_0 B_1 \rangle$, $\langle A_0 A_1 A_0 B_1 \rangle$ and the like.

As such, out of all the terms in the objective function, only ther terms $\langle A_x \rangle, \langle B_y \rangle$ and $\langle A_x B_y \rangle$ can be obtained from experimental data and substituted into the expression for the fidelity. However, the values of the other terms like $\langle A_0 A_1 B_0 B_1 \rangle$ are not available from experimental data. These will be treated as variables, which a computer program, known as a Semi-definite program or SDP, will vary until a solution for the minimum fidelity is found.

To perform a minimisation in this way, one needs to specify some form of constraint. Specifically, it would be ideal for the probability point to be no-signalling and to lie in the quantum set, Q. However, it turns out that there is no efficient way to to minimise over the quantum set Q directly. However, it is known that one can perform the minimisation over a superset relaxation of the actual quantum set, Q_l, instead. Such superset relaxations of the quantum set is such that they converge to the actual quantum set as the level l is increased[6]: $\lim_{l \to \infty} Q_l = Q$. This is illustrated in figure 6 on the next page.

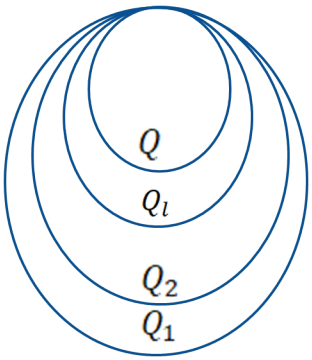

Figure 6: Illustration of the convergence of Q_l to Q as $l \to \infty$

To carry out the minimisation computationally, one first chooses some finite level l over which one performs the minimisation. Then, to impose that a probability point is within this superset relaxation Q_l of the quantum set Q, is equivalent to imposing that the moment matrix

$$\Gamma = \begin{pmatrix} 1 & A_0 & B_0 & \dots & A_0A_1 & B_0B_1 & \dots \\ A_0 & 1 & A_0A_1 & \dots & A_0B_1 & A_1 & \dots \\ B_0 & A_0A_1 & 1 & \dots & A_1B_1 & A_1A_0A_1 & \dots \\ \vdots & \vdots & \vdots & \vdots & \vdots & \vdots & \dots \\ A_1A_0 & A_1 & A_1A_0B_0 & \dots & 1 & A_1A_0B_0B_1 & \dots \\ \vdots & \vdots & \vdots & \vdots & \vdots & \vdots & \ddots \end{pmatrix}$$

is positive-semidefinite (eigenvalues≥ 0)[6, 3].

Here, the brackets denoting expectation values have been left out, but it should be understood that the elements of the matrix are all expectation values of the respective observables. Looking at the first row of the matrix, the expectation values of observables (moments) A_0, A_0B_0, A_0A_1 etc. are being listed from left to right. In the first column of the matrix, the exact same order of the *hermitian conjugate* of the observables in the first row is listed downwards. The matrix is then formed from taking an element from the first column and multiplying it with one element from the first row.

This matrix can be as large as one needs it to be, and its size depends on the level l, in Q_l, over which the minimisation is performed. l here represents the maximum number of observables multiplied to one another in any one of the elements of the first row/column. More succinctly, Q_1 contains the moments A_0, A_1, B_0, B_1. Q_2 then contains all the moments in Q_1 together with moments like A_0A_1, B_1B_0 and A_0B_0 that consists of two observables multiplied to one another, covering all possible combinations.

While there is no upper limit to the size of the matrix, there is a minimum size that one must use depending on the expression of the objective function(which is the fidelity in our case). The matrix must be large enough such that it contains all the variables in the objective function. Here, for instance, there is a term in the objective function that reads $\langle A_0A_1A_0B_0B_1B_0\rangle$, which neccesitates the inclusion of some moments in Q_3 in order to ensure that this term appears in the matrix Γ.

It is however, not necessary to include all the moments in Q_3; one can just keep adding moments and stop somewhere between Q_2 and Q_3, when all the necessary terms are in the matrix. The analysis presented in the following section (6), uses a matrix of size 21 by 21, the minimum size required to include all the necessary moments. That being said, as illustrated in figure 6, the larger the matrix, the smaller the set Q_l is. Therefore, if one goes to a higher level in the hierarchy (higher l), the minimisation is performed over a smaller set, and the result can only either be the same as before, or (hopefully) increase . This is useful if one desires to obtain better lower bounds on the fidelity.

The next step then, as mentioned earlier, is to minimise the objective function F subject to the constraint that the matrix Γ is positive semi-definite:

$$\text{Fidelity} = \min\ F \qquad \text{s.t} \quad \Gamma \geq 0 \tag{27}$$

This returns the minimum fidelity with the singlet state, given some observed values of $\langle A_x\rangle, \langle B_y\rangle$ and $\langle A_xB_y\rangle$ which were inserted into the matrix Γ. These values can be obtained from the experimental data $P(a, b|x, y)$ as demonstrated in section 5.2.

At this point, it is useful for one to check if the SDP works properly before proceeding further. To do so, one could substitute the values $\langle A_x B_y \rangle = (-1)^{xy} \frac{1}{\sqrt{2}}$ which correspond to $CHSH = 2\sqrt{2}$ into the matrix and run the program. This was carried out and the fidelity obtained was indeed 1, serving as a check that the objective function F was correct, and that the SDP was working correctly.

5.5 Regularisation: another SDP

In section 4.3, the idea of Regularisation was discussed, and the details of the procedure will be discussed here. Regularisation is used to project the experimental probability point into a set of correlations Q_l that obeys no-signalling. This is done by finding the point $\vec{P}_{NQA_2}$ that minimises the two norm distance from the experimental probability point $\vec{P}_{exp}(a, b|x, y)$:

$$\vec{P}_{NQA_2}(\vec{P}_{exp}) = \text{argmin}_{\vec{P} \in Q_l} \|\vec{P}_{exp} - \vec{P}\|_2 \tag{28}$$

The requirement that $\vec{P} \in Q_l$ is fulfilled by imposing that the appropriate moment matrix (as described in section 5.4) is positive semi-definite.

To perform this minimisation of the two-norm, another SDP is used. It turns out that one can reformulate equation (28) into following problem which can be solved using an SDP[4]:

$$\begin{aligned} &\text{argmin}_{\vec{P} \in Q_l} s \\ \text{s.t} \quad &\begin{pmatrix} s\mathbb{1} & \vec{P} - \vec{P}_{exp} \\ \vec{P}^T - \vec{P}_{exp}^T & s \end{pmatrix} \geq 0 \end{aligned} \tag{29}$$

Here, the $\mathbb{1}$ represents the 16x16 identity matrix, and $\vec{P} - \vec{P}_{exp}$ is a 16x1 column vector so that the matrix is a 17x17 square matrix. Note here that it is also necessary to run another SDP using the moment matrix described in section 5.4 to enforce the constraint that $\vec{P} \in Q_l$.

Although this section is discusssed after section 5.3, in practice the regularisation is done first, right after experimental data is obtained. The reason it is presented is that regularisation requires one to already be familiar with the content presented in section 5.4.

6 Application to data from a CHSH simulator

In this section, the data obtained from a CHSH simulator will be analysed using the techniques discussed so far. Regularisation will first be performed on the raw data obtained from the simulator before the lower bound on the fidelity is found. This will be done for different number of runs of the experiment and the results will be analysed.

6.1 The CHSH Simulator (perfect correlations)

The details of the simulator that generates the data for the CHSH scenario will be explained in this section. The simulator is programmed such that Alice and Bob choose their settings x, y completely randomly. In terms of the code for the simulator, we first generate two random numbers, one each for Alice and for Bob. If Alice's number is greater than 0.5, then the setting on Alice's side is set to $x = 1$, and otherwise it is set to $x = 0$. The same is done for Bob, effectively simulating the random choosing of settings.

Next, the simulator needs to be programmed to generate the correct outputs based on the settings. To do this, the probabilities $P(a, b|x, y)$ for the ideal case must first be known. In a bipartite scenario with binary settings, from section 5.2 equation (20) one has the following expression:

$$P(a, b|x, y) = \frac{1}{4}(1 + a\langle A_x\rangle + b\langle B_y\rangle + ab\langle A_x B_y\rangle)$$

To obtain data that maximally violates the CHSH inequality, the values $\langle A_x\rangle = \langle B_y\rangle = 0$, $\langle A_x B_y\rangle = \frac{1}{\sqrt{2}}(-1)^{xy}$ will be used as they lead to the maximal violation of $CHSH = 2\sqrt{2}$. As such, one obtains:

$$P(a, b|x, y) = \frac{1}{4}(1 + \frac{1}{\sqrt{2}}ab(-1)^{xy}) \tag{30}$$

First, consider the case where the settings are $(x, y) = (0, 0), (0, 1)$ or $(1, 0)$:

$$P(a, b|x, y) = \frac{1}{4}(1 + \frac{1}{\sqrt{2}}ab) \tag{31}$$

or, upon substituting the values of a and b,

$$P(++) = P(--) = \frac{1}{4}(1 + \frac{1}{\sqrt{2}})$$
$$P(+-) = P(-+) = \frac{1}{4}(1 - \frac{1}{\sqrt{2}})$$

Now, given the inputs $(x, y) = (0, 0), (0, 1)$ or $(1, 0)$, the simulator must be programmed to give the correct outputs a, b. Looking at the probabilities above, one can split them into two cases: $a = b$ and $a \neq b$:

$$P(a = b) = P(++) + P(--) = \frac{1}{2}(1 + \frac{1}{\sqrt{2}})$$
$$P(a \neq b) = P(+-) + P(-+) = \frac{1}{2}(1 - \frac{1}{\sqrt{2}})$$

We can first instruct it to determine which case the outputs will fall under($a = b$ or $a \neq b$). To that end, a random number r_1 is generated. If r_1 is greater than $P(a = b)$, then the outputs a and b will be different: $a = -1, b = 1$ or $a = 1, b = -1$. Otherwise, the outputs will be the same.

Lastly, to determine what the outputs are exactly, another random number r_2 is generated. In the case that $a \neq b$ is chosen using r_1, since $P(+-) = P(-+) = \frac{1}{4}(1 - \frac{1}{\sqrt{2}})$, the cases $a = 1, b = -1$ and $a = -1, b = 1$ are equally likely. Therefore, one imposes that if r_2 is greater than 0.5, then the simulator gives the outputs $a = 1, b = -1$. Otherwise, it gives $a = -1, b = 1$.

For the case where the settings $(x, y) = (1, 1)$, from (30), we have:

$$P(a, b|x, y) = \frac{1}{4}(1 - \frac{1}{\sqrt{2}}ab) \tag{32}$$

Similarly, one ends up with:

$$P(a = b) = P(++) + P(--) = \frac{1}{2}(1 - \frac{1}{\sqrt{2}})$$
$$P(a \neq b) = P(+-) + P(-+) = \frac{1}{2}(1 + \frac{1}{\sqrt{2}})$$

As before, a random number r_1 is generated to decide which case of the outputs ($a = b$ or $a \neq b$) it falls under . Accordingly, if $r_1 > P(a = b)$, we have the case $a \neq b$. Since $P(+-) = P(-+)$, a second random number r_2 is generated to decide which one of the two cases ($a = +1, b = -1$ or $a = -1, b = +1$) the output falls under as before.

6.2 Variation of Fidelity with Number of runs

In this section, the results of the application of the ideas presented in sections 5.1-5.5 to the data obtained from the *perfect* CHSH simulator described in section 6 will be presented. The data was first obtained from the simulator, and the probabilities were estimated: $P(a, b|x, y) = \frac{n(a,b|x,y)}{N}$. Here, $n(a, b|x, y)$ is the number of runs in which the outcomes a, b were obtained when the settings were x, y and N is the total number of runs performed. Regularisation was then performed on the estimated $P(a, b|x, y)$ before the SDP was run to obtain a lower bound on the fidelity. The number of runs N was varied, and the effect that had on the fidelity was investigated. The results are shown in the following graph:

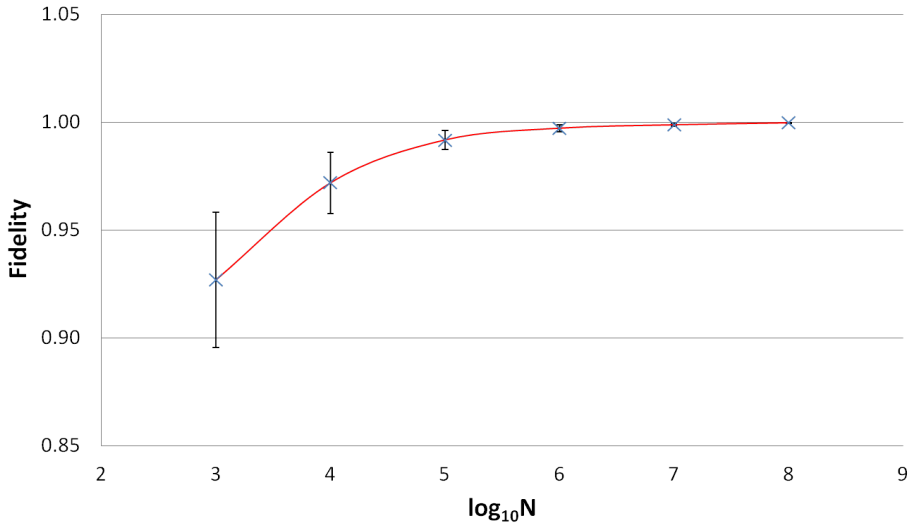

Figure 7: Graph of Minimum Fidelity against the Logarithm of the Number of Runs(N)

This is a plot of the fidelity with the singlet state against the logarithm of the number of runs of the experiment. Therefore, 3 on the x-axis represents 1000 runs and 4 represents 10,000 and so on. As mentioned earlier, the size of the matrix used in the SDP is 21 by 21, the minimum required size.

From the graph, we see that as the number of runs is increased, the average minimum fidelity improves and tends to 1 as more runs are taken. The standard deviation of the fidelity appears to become smaller as the number of runs is increased. This is expected since increasing the number of runs gives more data, which evens out statistical fluctuations and results in a smaller spread of data, and gives a more accurate measure of the actual fidelity. Therefore, ideally one should take as many runs as possible to obtain the best possible data. Practically however, one cannot keep going on forever, and needs to stop somewhere when actually performing the experiment. From figure 7, for $N = 1000$, the fidelity is less than 0.95, which suggests that the minimum one should aim for is perhaps $N \geq 10,000$, bearing in mind that this is a perfect simulator and one should be getting a fidelity close to 1.

6.3 Suspected errors caused by rounding

When plotting the graph in figure 6, an issue arose. In some runs of the SDP, the program failed to perform the optimisation given the constraints imposed. In principle, this should not have been the case, since the regularisation process would have taken care of projecting the point into Q_l over which the SDP performs the minimisation of the objective function.

One explanation for this error would be the rounding off that is done to the experimental data point after the regularisation is performed. Since a perfect CHSH simulator was used, it is possible that the probability point obtained was very close to the boundary of Q_l, where the point corresponding to $CHSH = 2\sqrt{2}$ lies. Hence, after some rounding off, the regularised point might have ended up lying on the outside of Q_l. Since the SDP demands that the probability point *must* lie in Q_l to begin with, it would explain why the program failed to perform the minimisation. This idea is illustrated in the diagram on the next page.

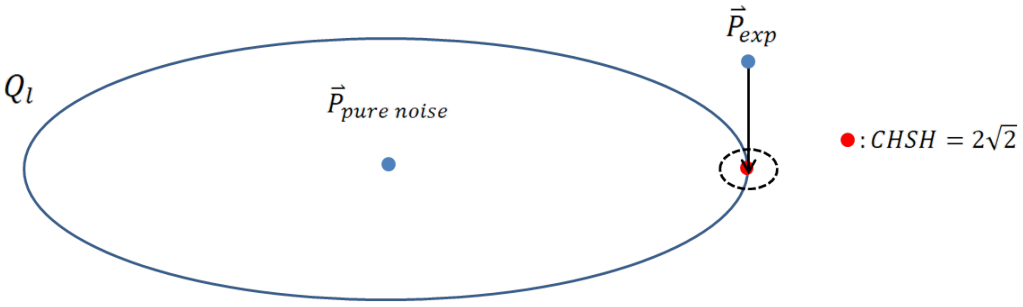

Figure 8: Errors from Rounding-off

In figure 8, the arrow represents the projection of $\vec{P}_{exp}$ into the the set Q_l, and the red point represents the probability point which gives the maximal violation of $CHSH = 2\sqrt{2}$. The small dotted circle here represents the rounding off of the final values after the projection, which according to the diagram, causes the projected point to lie outside Q_l about about half the time, leading to errors later when the SDP is run.

A consequence of this, then, would be that with increasing noise in the data, the failure rate from running the SDP should fall. The reasoning is as follows: First, note that the center of the set Q_l is a probability point, $\vec{P}_{pure\ noise}$, that represents 100% noisy data. Then, with less perfect data, the experimental probability point should move closer to the center of the set Q_l, which reduces (or even completely eliminates) instances where the rounding off causes the point to end up on the outside of Q_l. This is illustrated in the following diagram:

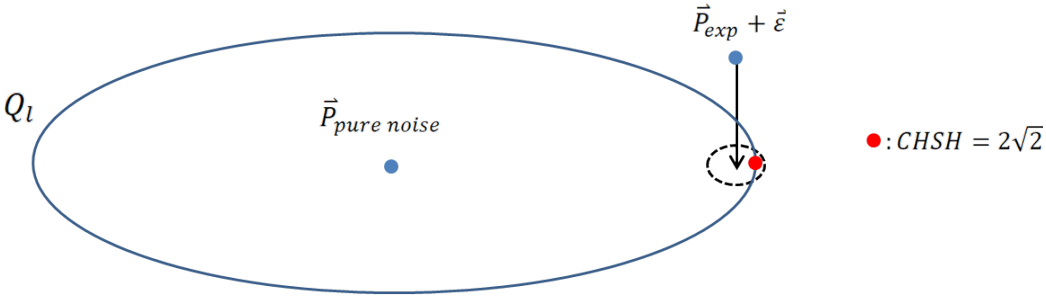

Figure 9: Lower error rate using noisy data

Here, the new probability point with some added noise $\vec{\epsilon}$ is brought closer towards the center of Q_l which causes most of the dotted circle (which represents the rounding) to lie within Q_l. In fact with enough noise, the experimental probability point would lie far enough towards the center of Q_l, and any rounding off would not cause the point to end up on the outside of Q_l. Therefore, we expect fewer, or even no instances of failed optimisations with increasing noise.

6.4 Adding noise to the simulator

To confirm if the previous conjecture was valid, noise was added to the simulator and data was collected to examine how the failure rate of the SDP changed with increasing noise. The addition of noise to the simulator will now be explained in detail.

From (30), we see that the perfect CHSH simulator will give the correlations $P_{CHSH}(a,b|x,y) = \frac{1}{4}(1 + \frac{1}{\sqrt{2}}ab(-1)^{xy})$. However, this expression will change if noise is accounted for. To obtain this new expression, consider the following state:

$$\rho = |\Phi^+\rangle \langle\Phi^+| (1-\epsilon) + \frac{\mathbb{1}}{4}\epsilon \tag{33}$$

This state here is known as a Werner State[3]. In this case it is essentially a mixture of the perfect singlet state ($|\Phi^+\rangle \langle\Phi^+|$) and white noise ($\frac{\mathbb{1}}{4}$), where ϵ is a small parameter which can be used to control the amount of noise. Now, the new correlations $P(a,b|x,y)$ that are obtained with the addition of noise are as follows:

$$\begin{aligned}
P(a,b|x,y) =& Tr(\rho \Pi_a^x \otimes \Pi_b^y) \\
=& Tr[(1-\epsilon)|\Phi^+\rangle \langle\Phi^+| \Pi_a^x \otimes \Pi_b^y + \frac{\mathbb{1}}{4}\epsilon \Pi_a^x \otimes \Pi_b^y] \\
=& (1-\epsilon) Tr(|\Phi^+\rangle \langle\Phi^+| \Pi_a^x \otimes \Pi_b^y) + \epsilon Tr(\frac{\mathbb{1}}{4}\Pi_a^x \otimes \Pi_b^y) \\
=& (1-\epsilon) P_{CHSH} + \epsilon P_{noise} \\
=& \frac{1}{4}(1 + \frac{1}{\sqrt{2}}ab(-1)^{xy})(1-\epsilon) + \frac{1}{4}\epsilon \\
=& \frac{1}{4} + \frac{(1-\epsilon)}{4}(-1)^{xy}\frac{ab}{\sqrt{2}}
\end{aligned} \tag{34}$$

Replacing the $P(a,b|x,y)$ expression in the simulator with this new expression, the amount of noise was varied and the changes in the number of failed optimisations from the SDP was examined. The SDP was run using 30 sets of data for each N (number of runs). The results are shown in figure 10 on the following page.

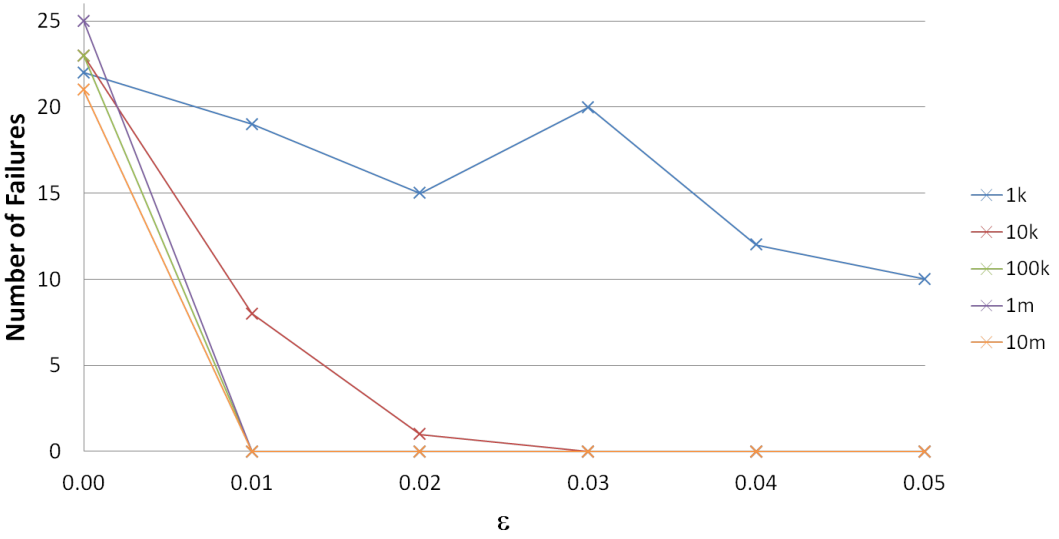

Figure 10: Variation of the Number of Failures with increasing noise ϵ for different number of runs

The general trend here is that the failure rate falls with increasing ϵ, in accordance with our suspicions. More interestingly, the failure rate drops to 0 very quickly the as more runs of the experiment is performed. For 100,000, 1 million, and 10 million runs, the number of failures drop to 0 immediately after a little noise is added. The trend for 10,000 runs is more gradual, while the trend for 1000 runs is erratic but nevertheless shows a decreasing trend. This is expected as a smaller number of runs generally give data with a larger spread, and therefore has a higher chance of falling outside of Q_l after regularisation. Also, if one does not take enough runs, it is even possible that with more noise, the failure rate increases as seen for $\epsilon = 0.03$ in the case of 1000 runs. This is due to the spread of data for the case of 1000 runs being too large as represented by the standard deviation in figure 7.

6.5 Variation of minimum fidelity with noise

As noise increases, one expects the fidelity of the state with the singlet to fall. To check if that was true, the fidelity was plotted against the noise ϵ, and the results are shown in the following graph. Each line in the following graph represents a different number of runs performed by Alice and Bob.

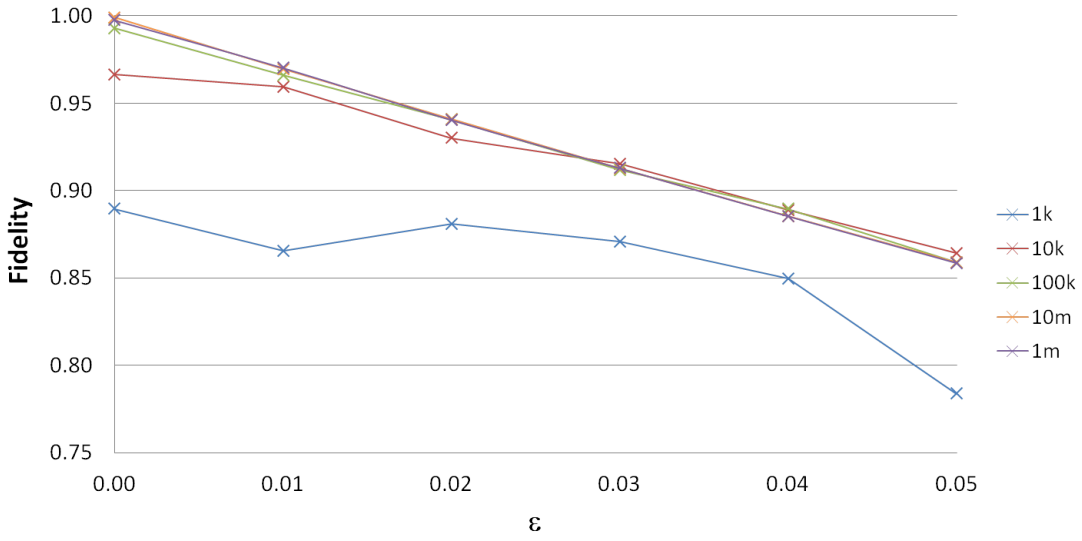

Figure 11: Variation of minimum fidelity with increasing noise ϵ for different number of runs

The graph depicted here is in fact the equivalent of the robustness curves described in sections 4.1 and 4.2. However, in this case, the noise is introduced in the simulator as described in section 6.4, instead of being added directly added to the perfect correlations as depicted in figure 2. This therefore more closely mimics the sort of data that would be obtained from an actual experiment.

The general trend shown in figure 11 is that the fidelity falls with increasing noise as one expects. More interestingly, however, is the shapes of the graphs obtained. The higher the number of runs, the more regular-looking the graphs become.

The data for 1000 runs gave the most erratic-looking graph, and upon comparing the data points for $\epsilon = 0.01$ and $\epsilon = 0.02$, we even see that the average fidelity increases, contrary to the expectation that it should fall. This is due in large part to the statistical fluctuations evident from the considerably large standard deviation seen in figure 7 for 1000 runs. Therefore, this spread of data becomes dominant enough to give imprecise results if one does not perform enough runs of the experiment.

Upon looking at the data for 10,000 runs, we see that it is still irregular in shape. However, at least a decreasing trend for the fidelity is observed, better than the results obtained from a 1000 runs. Increasing the number of runs, one observes that the graphs become increasingly regular, as the statistical fluctuations even themselves out with more runs, giving more precise data. This therefore, yet again, suggests that to obtain precise results, one ought to perform more than 1000 runs, and perhaps even more than 10,000.

Also, with a greater number of runs, one expects to get better lower bounds on the fidelity. This is indeed true for the case where there was no noise in the system (refer to figure 7). However, looking at figure 11, this is no longer true once noise was introduced. For $\epsilon = 0.02$, the average fidelities obtained from the data corresponding to 100,000, 1 million, and 10 million runs are roughly the same as the points are seen to be rather close to one another. Also, for $\epsilon = 0.03$, the average fidelity obtained from the data of 10,000 runs turned out to be higher than that of what was obtained with 100,000, 1 million and 10million runs.

To further examine this effect, the average fidelity, together with the standard deviation, was plotted against the logarithm of the number of runs ($\log_{10} N$) for a fixed amount of noise ϵ. The following graph is one such plot with noise $\epsilon = 0.01$

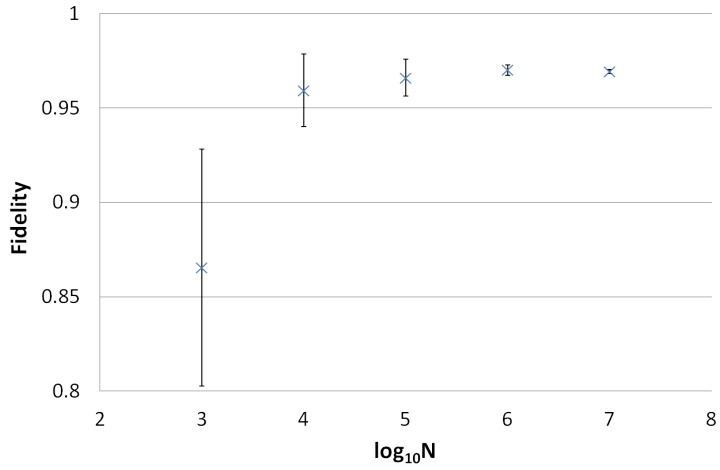

Figure 12: Variation of average fidelity with number of runs for $\epsilon = 0.01$

Here, we see that the fidelity increases with the number of runs, which is expected from the similar analysis done with the perfect case where there was no noise (figure 7), the difference here being that the fidelity no longer approaches 1 due to the addition of noise. Also, as observed earlier, the spread of the data for a small number of runs is considerably large, resulting in a comparatively large standard deviation which is especially prominent for the case where $N = 1000$.

The standard deviation becomes smaller with more runs as seen earlier, but the overlap between the standard deviations of different runs now becomes much more apparent when noise is added. Furthermore, the increase in the average fidelity with the number of runs is now less evident than before, and this is especially true for $N \geq 10,000$ as seen in the graph.

To further investigate this observation, another graph, now with more noise ($\epsilon = 0.03$), was plotted.

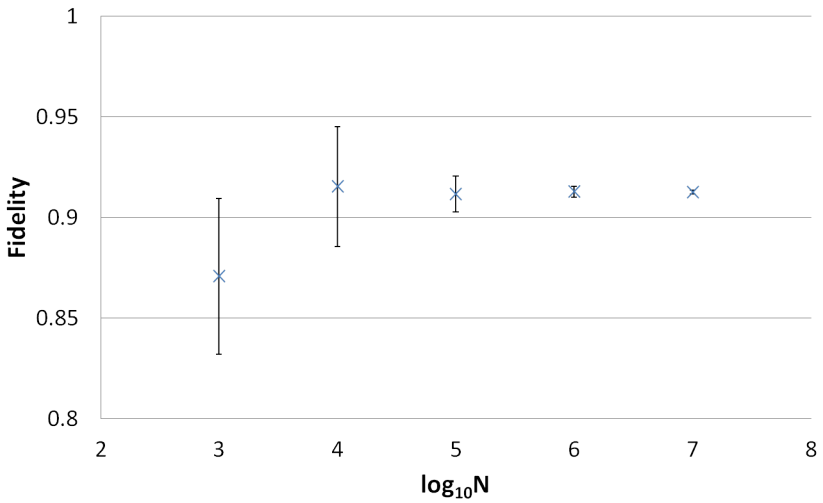

Figure 13: Variation of average fidelity with the number of runs (N) for $\epsilon = 0.03$

In this figure, we see that for $N \geq 10,000$ the average fidelity is now more or less the same. Therefore, increasing the number of runs here only serves to reduce the standard deviation, and has little effect on increasing the average fidelity when sufficient noise is present in the system.

6.6 Experimental Data from IBM

With the help of Professor Scarani's PhD student Goh Koon Tong, experimental data from running the CHSH experiment on the qubits from IBM Q Experience[12] was obtained. It returned a value of $CHSH = 2.2756$, and upon running the SDP as described in section 5.4 using a matrix of the same size as before, the fidelity obtained was $F = 0.5152$. This is only slightly better than the trivial bound of $F = 0.5$, and is due in large part to the noise present. This is depicted in the following graph:

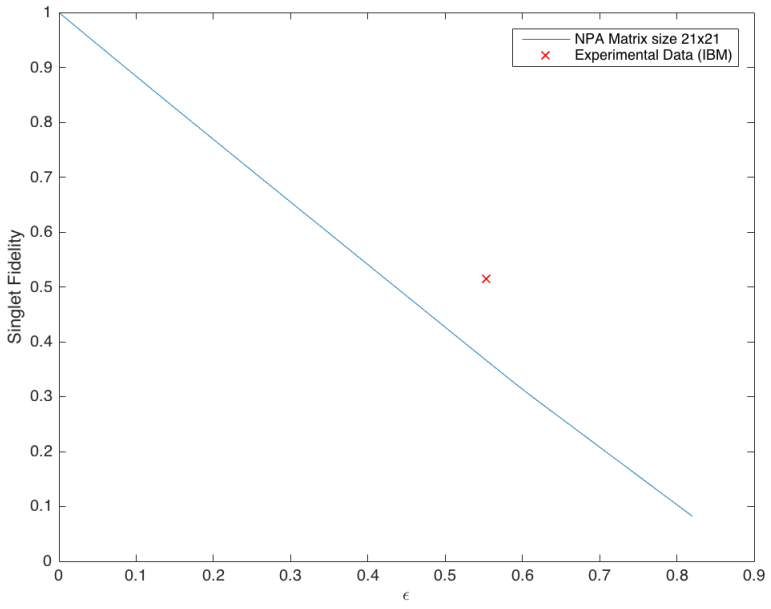

Figure 14: Fidelity obtained from IBM data

An interesting point to note here is that when using the CHSH value to self-test, one obtains the minimum possible fidelity given some $CHSH = 2\sqrt{2} - \epsilon$. However, in experiments, the full statistics $P(a, b|x, y)$ are available, and therefore can be used directly to find the lower bound on the fidelity. In this case, if only the CHSH value was considered, the resulting fidelity would be $F = 0.5$, a trivial bound. However, since the full statistics were available, the lower bound obtained was slightly higher, at $F = 0.5152$.

7 Future Work

The tools used in discussion so far are general approaches that can be applied to other self-testing scenarios if one wishes to perform analysis using real experimental data. In this section, the particular scenario of two singlets will be discussed. It is known as the double-CHSH scenario as it uses very similar ideas as in the one singlet case that has been discussed so far.

7.1 The Setup and Notation

In this double-CHSH scenario, we have two parties Alice and Bob, and two boxes as before(refer to figure 2.1). However, instead of having binary settings and binary outputs as before, each party now has access to four possible measurement settings, $x, y \in \{0, 1, 2, 3\}$ and each setting now gives four possible outcomes $a, b \in 0, 1, 2, 3$. Therefore, the correlations $P(a, b|x, y)$ obtained has $4^4 = 256$ entries, up from just 16 in the one singlet case.

Ideally, one desires to self test two singlets shared by Alice and Bob. This means that in the ideal case, Alice and Bob both have two qubits each. Each of the qubits Alice has is entangled with the corresponding qubit that Bob has. In other words, the combined state of the entire system takes the form $|\bar{\psi}\rangle_{AB} = |\Phi^+\rangle_{A_I B_I} \otimes |\Phi^+\rangle_{A_{II} B_{II}}$.

Since both parties now have two qubits each, for the sake of clarity, one ought to specify each qubit with the use of some additional notation[7]. Consider the following setup below:

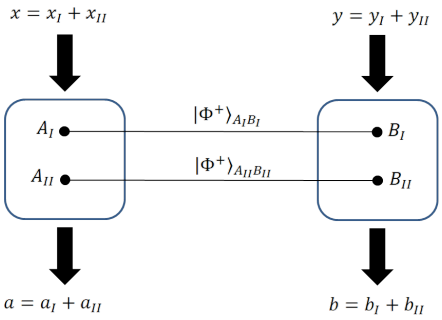

Figure 15: Notation for the two singlet scenario

Alice's first qubit is denoted by A_I and her second qubit is denoted by A_{II}, and the same applies for Bob. The qubits A_I and B_I are entangled and are in the singlet state $|\Phi^+\rangle_{A_I B_I}$, and the same is true for the system denoted by A_{II} and B_{II}. The settings in this scenario are broken up into two components (x_I and x_{II}), where $x_i \in \{0, 1\}$ and $x = 2x_I + x_{II}$. Note that while the notation here is slightly different from was what used before in section 3.5, it is only a matter of how one labels the outcomes.

This construction is motivated by the one singlet case, where $x \in \{0, 1\}$ is taken as an input for Alice's box (which only had 1 qubit), and $a \in \{0, 1\}$ is obtained as an output. Here, the scenario is exactly the same, just that there are two qubits instead of one. Therefore, the qubit A_I takes the input x_I and gives the output a_I, both of which are binary, and the same applies to qubit A_{II}. To relate this to the actual setting that Alice inputs, one then has the relation $x = 2x_I + x_{II}$. The combination of possible inputs are shown in the table below:

x_I	x_{II}	x
0	0	0
0	1	1
1	0	2
1	1	3

From the table, Alice inputting $x = 1$, actually corresponds to her inputting $x_I = 0$ into the first qubit A_I and x_{II} into the second qubit A_{II}. In a similar fashion, if Alice obtains $a = 0$ for his particular run, then it corresponds to qubit A_I giving the output $a_I = 0$ and qubit A_{II} giving the output $a_{II} = 0$. This description is identical on Bob's end. Note that the main difference here is that for each input setting x, Alice can obtain one of 4 possible outcomes, $a \in \{0, 1, 2, 3\}$, instead of the binary outcomes in the one singlet case.

7.2 The Moment Matrix and the Observed Correlations

As in section 5.4, the construction of the moment matrix and the imposition that it is positive semi-definite is necessary to carry out the optimisation using an SDP. In this scenario however, for each of Alice's settings, there are 4 outcomes. Therefore, the use of observables like A_x, B_y will no longer be possible since they only give binary outcomes. Therefore, the moment matrix needs to be

constructed using projectors $\Pi_{a|x}$ and $\Pi_{b|y}$ instead. Also, the isometry used here is

As before, the matrix is constructed based on the level l that is required. Q_1 contains the moments of just single projectors $\{\Pi_{a|x}, \Pi_{b|y}\}$, while Q_2 contains the moments in Q_1 together with the combinations of the product of two projectors $\{\Pi_{a|x}\Pi_{a'|x'}, \Pi_{a|x}\Pi_{b|y}...\}$ and so on. With that, the observed correlations $P(a, b|x, y) = \langle \Pi_{a|x} \otimes \Pi_{b|y} \rangle$ are inserted into the matrix, and the optimisation to find the minimum fidelity is then performed. The objective function here can be obtained using a similar swap isometry[5, 7] as used in section 5.1, but now accounting for the extra qubits and ancillas required.

8 Conclusion and Summary

In this section, a brief summary of Self-Testing, Robustness curves, Regularisation and other relevant ideas covered in this report will be presented. Also, the results of the application of these techniques on simulated and experimental data will also be summarized.

8.1 The Main Ideas

Self-Testing in essence refers to the fact that one can identify a unique state and compatible measurements made on that state just simply by the observation of the correlations $P(a, b|x, y)$. This is a device independent approach as no assumptions are made on the inner workings of the boxes Alice and Bob possess, and conclusions are drawn purely from the correlations. The statistic $CHSH = 2\sqrt{2}$ for instance, allows one to conclude Alice and Bob must share singlet state with the corresponding sigma matrices being the measurements performed.

However, such an identification only works in the perfect case, where the correlations observed are exactly the perfect ones known to self-test the state. Therefore, to make this practical, one needs to be able to draw conclusions about the state, given that non-ideal correlations (due to experimental imperfections and statistical errors) are observed. This is where robustness curves come in. These curves provide one with the minimum fidelity (or overlap) a state (which the observed correlations are obtained from) shares with the ideal state (which the ideal correlations are supposed to self test).

Even with these tools, it turns out that one is still not yet ready to perform any analysis on raw experimental data. The reason is that self-testing and robustness bounds assume that the no-signalling condition *always* holds, which is most of the time, not true for raw data. Therefore, one must first regularise the data so that the no-signalling conditions are fulfilled before performing the minimisation of the fidelity using an SDP.

In this report, a regularisation procedure was applied to data obtained from a simulator, and the change in the resulting fidelity due to different number of runs of the experiment was investigated. Also, to obtain data that mimics what one might obtain from the lab, noise was added to the simulator. The changes in the resulting fidelities (after regularising the data) due to both the increase

in noise as well as the increase in the number of runs of the experiment was examined.

8.2 The Results Obtained

8.2.1 Variation of the minimum fidelity with number of runs of the experiment

Using a perfect CHSH simulator designed to give data that would give $CHSH = 2\sqrt{2}$, the variation of the minimum fidelity with the number of runs of the experiment was investigated (See figure 7). In accordance with initial expectations, the minimum fidelity increased as more runs were taken. Also, the standard deviation decreased as the number of runs was increased. This is due to the fact that the statistical fluctuations even out, leading to a smaller spread in data.

8.2.2 Optimisation failures and variation with noise

Upon attempting to run the SDP on regularised data, it was observed that some of the optimisations failed. The suspected reason was that the rounding-off that occurred during the regularisation might have caused the point to fall outside of the set of correlations that obey the no-signalling condition. To check if this was the case, noise was added to the simulator, with the intuition being that more noise would pull the point further into the set and give less optimisation errors. The change in the number of failed optimisations with increasing noise was examined, and this was done for different number of runs (See figure 10).

The results confirm the initial suspicions, since with increasing noise, the failure rate falls. Additionally, for a larger number of runs, the failure rate falls to zero very quickly. This is also expected since a smaller spread of data is obtained and only a little noise is needed to completely pull it into Q_l.

8.2.3 Variation of minimum fidelity with noise

As in typical robustness curves, the change in minimum fidelity (after regularisation) with increasing noise was examined for different number of runs of the experiment (See figure 11). The general trend observed is that the fidelity falls with increasing noise, as expected. However, with a relatively small

number of runs ($\sim 10^3$) the variation of the fidelity is erratic and even gives counter-intuitive results. From the graphs obtained, it suggests that one ought to a take a much larger number of runs, at least ($\sim 10^4$) or higher in order to achieve more precise results.

Also, to more closely examine the effect noise had on the average fidelity and the standard deviation, two graphs corresponding to two different values of noise, $\epsilon = 0.01$ and $\epsilon = 0.03$ were plotted. It was observed that with increasing noise, increasing the number of runs only served to reduce the standard deviation, and not the average fidelity. Therefore, the advantage of taking more runs diminishes as more noise is added to the system.

8.3 Data from IBM

With the data obtained from running the CHSH experiment on IBM's Q experience, a CHSH value of $CHSH = 2.2756$ and a lower bound fidelity of $F = 0.5152$ was obtained, which is unfortunately only slightly higher than the trivial bound of $F = 0.5$. This was largely due to the inherent noise present in the IBM system.

References

[1] M.McKague, T. H. Yang, and V. Scarani. *Robust self-testing of the singlet.* J. Phys. A: Math. Theor. 45 455304 (2012) arXiv:1203.2976 [quant-ph]

[2] J. F. Clauser, M. A. Horne, A. Shimony, and R. A. Holt. *Proposed Experiment to Test Local Hidden-Variable Theories* Phys. Rev. Lett. 23, 880 (1969).

[3] V. Scarani. *The device-independent outlook on quantum physics* Acta Physica Slovaca 62, 347 (2012) arXiv:1303.3081 [quant-ph]

[4] P. S Lin, D. Rosset, Y. Zhang, J. D. Bancal, Y. C. Liang. *Device-independent point estimation from finite data and its application to device-independent property estimation* Phys. Rev. A 97, 032309 (2018) arXiv:1705.09245 [quant-ph]

[5] J. D. Bancal, M. Navascues, V. Scarani, T. Vertesi, T. H. Yang *Physical characterization of quantum devices from nonlocal correlations* Phys. Rev. A 91, 022115 (2015) arXiv:1307.7053 [quant-ph]

[6] M. Navascues, S. Pironio, A. Acin. *A convergent hierarchy of semidefinite programs characterizing the set of quantum correlations* New J. Phys. 10, 073013 (2008) arXiv:0803.4290 [quant-ph]

[7] X. Wu, J. D. Bancal, M. McKague, V. Scarani *Device-independent parallel self-testing of two singlets* Phys. Rev. A 93, 062121 (2016) arXiv:1512.02074 [quant-ph]

[8] Y. Wang, X. Wu, V. Scarani. *All the self-testings of the singlet for two binary measurements* New J. Phys. 18, 025021 (2016) arXiv:1511.04886 [quant-ph]

[9] K. T. Goh, J. Kaniewski, T. Vertesi, X. Wu, Y.C. Liang, V. Scarani. *Geometry of the set of quantum correlations* Phys. Rev. A 97, 022104 (2018) arXiv:1710.05892 [quant-ph]

[10] I. Chuang, M. Nielsen. *Quantum Computation and Quantum Information.* Cambridge University Press (2010).

[11] V. Scarani. *Quantum information: primitive notions and quantum correlations.* (2009) arXiv:0910.4222 [quant-ph]

[12] IBM Q Experience.
https://quantumexperience.ng.bluemix.net/qx/experience